Tuning Passive Mechanics through Differential Splicing of Titin during Skeletal Muscle Development

Coen A. C. Ottenheijm,[†§] Anna M. Knottnerus,[†] Danielle Buck,[†] Xiuju Luo,[†] Kevin Greer,[‡] Adam Hoying,[†] Siegfried Labeit,[¶] and Henk Granzier[†*]

[†]Department of Physiology, [‡]Bio5 Institute, University of Arizona, Tucson, Arizona; [§]Laboratory for Physiology, Institute for Cardiovascular Research, VU University Medical Center, Amsterdam, The Netherlands; and [¶]Medical Faculty Mannheim, University of Heidelberg, Mannheim, Germany

ABSTRACT During postnatal development, major changes in mechanical properties of skeletal muscle occur. We investigated passive properties of skeletal muscle in mice and rabbits that varied in age from 1 day to ~1 year. Neonatal skeletal muscle expressed large titin isoforms directly after birth, followed by a gradual switch toward progressively smaller isoforms that required weeks-to-months to be completed. This suggests an extremely high plasticity of titin splicing during skeletal muscle development. Titin exon microarray analysis showed increased expression of a large group of exons in neonatal muscle, when compared to adult muscle transcripts, with the majority of upregulated exons coding for the elastic proline-glutamate-valine-lysine (PEVK) region of titin. Protein analysis supported expression of a significantly larger PEVK segment in neonatal muscle. In line with these findings, we found >50% lower titin-based passive stiffness of neonatal muscle when compared to adult muscle. Inhibiting 3,5,3′-tri-iodo-L-thyronine and 3,5,3′,5′-tetra-iodo-L-thyronine secretion did not alter isoform switching, suggesting no major role for thyroid hormones in regulating differential titin splicing during postnatal development. In summary, our work shows that stiffening of skeletal muscle during postnatal development occurs through a decrease in titin isoform size, due mainly to a marked restructuring of the PEVK region of titin.

INTRODUCTION

Major changes in biomechanical characteristics in skeletal muscle take place during postnatal development, as reflected in adaptations in expression of isoforms of many of the proteins that make up the contractile machinery (1). Changes in proteins that determine passive stiffness have been poorly investigated. Muscle stiffness has important functional consequences in terms of movement control, and thus changes in passive stiffness during development need to be well understood. It is known that the stiffness of the musculo-tendon complex increases with age and body size (2,3) due to stiffening of tendons (4–6), but it is unclear to what extent titin, a major determinant of intracellular passive tension (7), is involved. A potential role for titin is suggested by previous work that showed an increase in resting tension of differentiating skeletal muscle fibers of the rat (8). Titin is a giant protein (~3–4 MDa) that is considered the third filament of the sarcomere, after the thick and thin filaments (9). Titin N-terminus is anchored in the Z-disc and its C-terminus extends to the M-line region of the sarcomere. The A-band region of titin is inextensible due to its interaction with the thick filament whereas the majority of the titin I-band region is extensible and functions as a molecular spring. This spring maintains the precise structural arrangement of thick and thin filaments (10) and gives rise to the passive stiffness of stretched sarcomeres (7).

In this study, we focused on skeletal muscle development and studied the remodeling of titin's spring region that is comprised of serially linked immunoglobulin (Ig)-like domains that make up the so-called tandem Ig segments, and a segment that is rich in proline-glutamate-valine-lysine (PEVK) residues (11). Titin is encoded by a single gene containing 363 exons in humans (12) and 358 exons in the mouse (13); alternative splicing leads to isoforms with distinct spring compositions (12). During cardiac development large compliant fetal titin isoforms switch to smaller stiff adult isoforms (14–17). Thus, titin is considered an adjustable molecular spring, with mechanical properties that can be tuned according to the mechanical demands placed on muscle. We characterized the titin isoforms expressed in various skeletal muscles of rabbit and mouse at ages that ranged from 1 day to ~1 year, using transcript, protein, and functional techniques. In addition, we studied the muscle ankyrin repeat proteins (MARPs), which bind to titin's extensible region, because recent knock-out studies showed that when MARPs are absent, skeletal muscle has reduced passive stiffness and expresses larger titin isoforms (18), suggesting that MARPs could play a role in the changes during development in passive mechanical behavior of muscle. We also studied whether reducing thyroid hormone levels impact on differential splicing of skeletal muscle titin during development. These experiments were motivated by recent work on titin expression in adult rat hearts (19) and cell culture studies with rat cardiac myocytes (17) that

Submitted February 18, 2009, and accepted for publication July 24, 2009.

Coen A. C. Ottenheijm and Anna M. Knottnerus contributed equally to the work.

*Correspondence: granzier@email.arizona.edu

Editor: Malcolm Irving.

0006-3495/09/10/2277/10 $2.00

doi: 10.1016/j.bpj.2009.07.041

indicate that thyroid hormones alters splicing of cardiac titin. Our results implicate different mechanisms during skeletal muscle postnatal development that allow for an intriguing degree of titin isoform diversity.

METHODS

Tissue harvesting

BL6 mice and New Zealand White rabbits of various ages (ranging from 1 day to ~1 year old) were anesthetized using isoflurane and the musculus quadriceps, gastrocnemius, tibialis cranialis (TC), extensor digitorum longus (EDL), and soleus were dissected. For transcript studies, muscles were dissected (1 day, and 105 days old) and stored in RNAlater (Ambion, Austin, TX). For gel-electrophoresis studies, muscles were quick-frozen in liquid nitrogen and stored at −80°C. All animal experiments were approved by Institutional Animal Care and Use Committee and followed the National Institutes of Health Guidelines, "Using Animals in Intramural Research", for animal use.

Gel-electrophoresis

For titin mobility studies, sodium dodecyl sulfate (SDS)-agarose electrophoresis was carried out as described previously (20). Briefly, muscle samples were pulverized to a fine powder and then rapidly solubilized and analyzed by vertical SDS-agarose electrophoresis (gastrocnemius homogenates contained a mixture of both the superficial white layers as well as the deep red layers). For estimation of molecular mass (M_r) of titin isoforms, the samples of interest were coelectrophoresed together with human soleus and left ventricle samples as these contain titin, nebulin and myosin heavy chain (MHC) isoforms of known sizes (human soleus titin T1: 3.82 MDa; nebulin: 773 kDa, respectively, and human left ventricle (LV) N2B T1: 2.97 MDa) (M_r from Labeit and Kolmerer (21,22)). Because migration distance in the gel scales with the logarithm of M_r, we could estimate the M_r of the proteins based on their migration distance, as shown previously (7,20). For some muscle samples from 1 day old animals, the titin M_r was similar to that of human soleus and appeared as one band in these gels. To estimate titin M_r from these samples, human soleus and LV were run adjacent to the sample of interest.

For determination of the time course of titin size transition during development, we quantified titin mobility by mixing samples of interest with chicken pectoralis, providing two constant mobility markers in the form of chicken pectoralis T1 and chicken pectoralis nebulin (see Fig. 2 *A* for further explanation). This relative titin size was plotted against animal age and fitted with a mono-exponential decay function. For determination of the total titin/MHC ratio the integrated optical density of total titin and MHC were determined as a function of the volume of solubilized protein sample that was loaded (a range of volumes was loaded on each gel). The slope of the linear range of the relation between integrated optical density and loaded volume was obtained for each protein. For determination of myosin heavy chain isoform composition, quick-frozen soleus samples were placed in SDS sample buffer containing 62.5 mM Tris-HCL, 2% (w/v) SDS, 10% (v/v) glycerol, and 0.001% (w/v) bromophenol blue at a pH of 6.8, and denatured by boiling for 2 min. The stacking gel contained a 4% acrylamide concentration (pH 6.7), and the separating gel contained 7% acrylamide (pH 8.7) with 30% glycerol (v/v). Control samples of mouse soleus and TC muscle were run on the gels for comparison of migration patterns of the myosin heavy chain isoforms. Sample volumes of 10 μL were loaded per lane. The gels were run for 24 h at 15°C and a constant voltage of 275 V. Gels were Coomassie-blue stained, and were scanned and analyzed with One-D scan EX (Scanalytics, Rockville, MD) software.

Western blotting

See the Supporting Material for a detailed description of the Western blotting methods.

Passive tension characteristics

The procedures for skinned muscle contractility were as described previously (7,23) with minor modifications. See the Supporting Material for a detailed description.

Transcript studies

See the Supporting Material for a detailed description of the transcript studies.

Thyroid hormone levels

For determination of baseline thyroid hormone levels, blood was removed from control mice at day 5, 10, 16, 20, 25, and 40, and centrifuged at 4°C. Serum was analyzed for 3,5,3′-tri-iodo-L-thyronine (T3), and 3,5,3′,5′-tetra-iodo-L-thyronine (T4) content by Antech Diagnostics (Morrisville, NC). Pharmacologically-induced congenital hypothyroidism was achieved as described previously with minor modifications (24). Briefly, 0.2% 2-mercapto-1-methylimidazole (MMI; Sigma-Aldrich, St. Louis, MO) was administered to the drinking water of pregnant BL6 mice, starting at day 10 of gestation. From birth until day 16 (the day of sacrifice) all animals were provided only drinking water with MMI.

Statistical analysis

For muscle mechanics experiments, typically 3–4 muscle preparations were studied per mouse with 5–6 mice per group. For the transcript and Western blotting studies typically five mice were analyzed per group. The data are presented as mean ± SE. Statistical analyses were carried out by *t*-test between neonatal and control mice; $p < 0.05$ was considered statistically significant.

RESULTS

Titin isoform switch during skeletal muscle development

To study titin isoform expression during skeletal muscle development we used SDS-agarose gel analysis of muscles from mice and rabbits of various ages. All samples showed well-resolved T1 and T2 titin bands (T1 is the full-length molecule and T2 a large degradation product comprising mainly the A-band segment of titin, which in most samples was barely detectable). A consistent finding in both species and in all muscle types studied (soleus, TC, EDL, gastrocnemius, and quadriceps) was slower migrating titin (T1) in neonatal samples (Fig. 1 *A*). To estimate the M_r of the neonatal and adult titin isoforms, we coelectrophoresed the neonate and adult samples of interest together with titin, nebulin, and MHC of known sizes, and used for this human soleus (T1: 3.82 MDa; nebulin: 773 kDa; MHC: 223 kDa, respectively; note that some muscles also had a lower MHC band and that although using the upper or lower MHC band had a negligible effect on the outcome, the upper band was used for consistency) and human left ventricle (N2B T1: 2.97 MDa; α-MHC: 223 kDa, M_r from Labeit and Kolmerer (21,22)). In neonatal tissue, titin was largest in murine quadriceps (3.89 MDa) and rabbit soleus (3.92 MDa), and in both mouse and rabbit titin was smallest in adult TC (3.24 and 3.34 MDa, respectively) (Fig. 1 *B*).

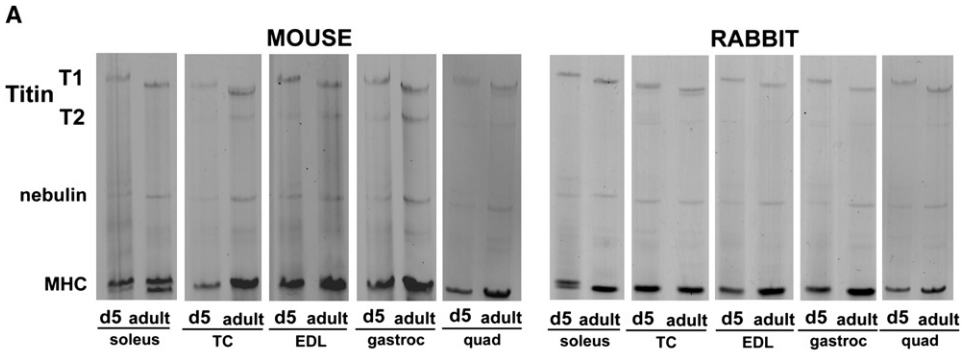

B

Titin isoform M_r estimates (MDa)

	mouse			rabbit		
Muscle	neonate	adult	*ΔMw*	neonate	adult	*ΔMw*
soleus	3.81	3.69	*0.12*	3.92	3.70	*0.22*
TC	3.77	3.24	*0.53*	3.67	3.34	*0.33*
EDL	3.68	3.57	*0.11*	3.80	3.56	*0.24*
gastrocnemius	3.66	3.51	*0.15*	3.85	3.53	*0.32*
quadriceps	3.89	3.51	*0.38*	3.90	3.41	*0.49*

TC and murine quadriceps (and on very rare occasions gastrocnemius) had sometimes a minor band; values shown represent the major band that was always present (see text for details).

FIGURE 1 (*A*) SDS-agarose gel electrophoresis of skeletal muscle from mouse (*left panel*) and rabbit (*right panel*) of day 5 (d5) and adult animals. In both species, and all muscle studied, neonatal muscle expressed a slower migrating titin isoform. T1, full length molecule; T2, degradation product, containing mainly titin's A-band segment; Gastroc, m. gastrocnemius; TC, m. tibialis cranialis; EDL, m. extensor digitorum longus; quad, m. quadriceps. (*B*) Estimated M_r of titin isoforms (in MDa) in neonatal and adult skeletal muscles (values obtained by coelectrophoresing the samples of interest with titin, nebulin, and MHC isoforms of known sizes (see Methods for details).

A consistent finding was that within muscle types, titin isoform size was larger in rabbits than in mice, both in adults and neonates (with the exception of neonatal TC, and adult EDL and quadriceps).

To investigate the time course of the titin isoform switch we evaluated titin migration using animals that varied in age from 1 day to ~1 year. Because there is a slight gel-to-gel variation in migration patterns we quantified titin mobility by mixing samples of interest with chicken pectoralis, providing two constant mobility markers in the form of chicken pectoralis T1 (M_r 3.0 MDa (13)), and chicken pectoralis nebulin that were used to define relative titin size as shown in Fig. 2 *A*, *inset*. Thus, relative titin size was defined as the ratio of *A* (the distance between T1 of the muscle of interest and chicken pectoralis nebulin) and *B* (the distance between T1 and nebulin of chicken pectoralis). The obtained values for relative titin size were insensitive to gel-to-gel variation (as determined by using identical samples on gels that were electrophoresed for greatly differing times). Fig. 2 *A* shows time course results for mouse (*left*) and rabbit (*right*). A surprising finding was that, with the exception of mouse TC and quadriceps, all muscle types only expressed a single titin isoform that gradually decreased in size (i.e., increased in mobility) suggesting a wide range of isoform sizes (see also Discussion). The expression pattern of mouse TC and quadriceps is more complex. In TC, after birth there is initially a single large isoform that within several days decreases in size and that later during development (~day 75) disappears. In TC of mice older than ~5 days an adult size isoform is also found that initially is coexpressed with neonatal titin, and after ~75 days is the sole isoform (Fig. 2, TC, *left panel*). In murine quadriceps, initially only a single isoform is expressed that decreases in size during development and remains of constant size in adults starting at ~100 days, at which age a second adult titin isoform of lower molecular mass is expressed (Fig. 2, quadriceps, *left panel*, *light gray diamonds*).

In all muscle types the neonatal to adult titin isoform transition can be fit well with a mono-exponential decay function (R^2 typically >0.9). The fits were used to derive the half transition time ($T_{1/2}$) from neonatal to adult titin (Fig. 2 *B*). The fastest transition occurred in soleus of rabbit ($T_{1/2}$ 5 days) and slowest in TC of rabbit ($T_{1/2}$ 30 days). Times for the same muscle type in different species varied and although $T_{1/2}$ times in rabbit tended to be longer, the difference was not significant.

To examine whether the change in titin isoform size during development is triggered by birth or instead already starts in utero, we determined relative titin size in E16 and E18 murine quadriceps (gastrocnemius, TC, soleus, and EDL were too small at E16 to isolate as a single muscle) and found that titin size in the embryonic tissue was comparable to early neonatal tissue (Fig. 2, quadriceps, *left panel inset*).

T2 titin was just detectable in most mouse tissues, but undetectable in mouse soleus and the vast majority of rabbit muscles. When measurable, the T2/T1 ratios were ~0.2 on average, and were independent of age, muscle type, and species. We also measured the titin/myosin (MHC) ratio for the various muscle types at different ages in the two species. The large variation in the titin/MHC ratios

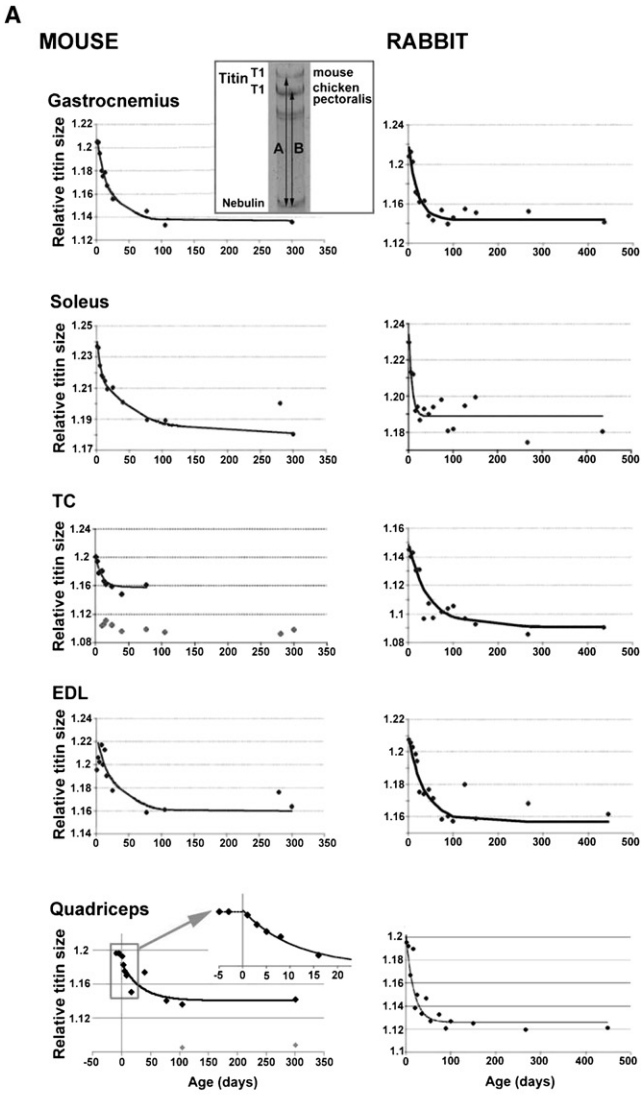

B

Muscle	Half-Transition time (days) Mouse	Rabbit
soleus	17	5
TC	6	30
EDL	17	25
gastrocnemius	13	14
quadriceps	17	12

FIGURE 2 (*A*) Relative titin size as a function of age. To correct for slight gel-to-gel variations in migration patterns we quantified titin mobility by mixing samples of interest with chicken pectoralis, providing two constant mobility markers in the form of chicken pectoralis T1 and chicken pectoralis nebulin that were used to define relative titin size as the ratio of A/B (inset shows typical gel-result for neonatal gastrocnemius, and illustrates how A and B were determined). The neonatal to adult isoform transition was fit with a mono-exponential decay function. Note the decrease in titin isoform size with increasing age. For murine TC and quadriceps, only the large neonatal titin isoform that decreased in size over time was analyzed (see also text). Murine quadriceps, *inset*: analysis of embryonic tissue (E16 and E18) showed titin isoform size to be comparable between embryonic and early neonatal tissue. (*B*) Table showing the half-transition time of the titin isoform switch during skeletal muscle development (half-transition time obtained from the mono-exponential decay function and defined as time-constant of fit times ln2).

(Fig. 3), especially in the neonatal samples, might reflect biological variation, but also the challenging nature of quantitative gel analysis, especially when analyzing degradation-sensitive proteins like titin. The expression ratio, averaged over all ages, was 0.22 ± 0.01 and this ratio was not different between muscle types or species.

In summary, the gel-electrophoresis studies indicate that titin isoform size decreases during skeletal muscle development, and that this transition from neonatal to adult takes place during the first weeks–months after birth.

Restructuring of titin spring region during postnatal development

To study whether the change in titin isoform size during skeletal muscle development is due to altered expression of specific titin domains, we used a mouse titin exon microarray that represents all of the 358 mouse titin exons (see the Supporting Material for an example of a microarray chip hybridized with cDNA). Experiments were carried out on gastrocnemius, TC, and quadriceps muscles from adult and neonatal mice (day 1). Results are shown in Fig. 4, *left*, color coded with exons upregulated in the neonate by >2-fold in red and downregulated by >2-fold in green. The *p*-values for each exon are also shown with the $p = 0.05$ and 0.01 levels indicated by broken lines in Fig. 4, *right*. In all three muscle types many upregulated exons were found, a small group of which in TC muscle consisted of Ig domains that are part of the proximal tandem Ig segment but the majority of which in all muscle types were localized in the PEVK region of titin (Fig. 4) (microarray studies on day 5 soleus (at day 1, soleus was too small for these experiments) showed significant upregulation of PEVK exons as well, data not shown). Thus, the spring region is a prime site for differential splicing during neonatal development, and elevated expression of PEVK domains is an important contributor to the lower electrophoretic mobility of neonatal titin (see Fig. 1).

To test for elevated expression of PEVK at the protein level, we used the anti-titin antibody 9D10 (previous work showed that 9D10 exclusively labels the PEVK segment from close to its N-terminal end to its C-terminal (25,26)). Consistent with our transcript data, Western blotting studies with 9D10 showed that relative to total titin (obtained from the PonceauS stained blot) expression of PEVK domains is upregulated in neonatal compared to muscle (Fig. 5). Moreover, we compared 9D10 staining between different adult skeletal muscles to test whether the differences in M_r between the small titin isoform in TC versus the larger isoforms in soleus, gastrocnemius and EDL are due to the TC having a relatively short PEVK segment. Normalized to TC, the 9D10/total titin ratio for EDL, soleus, and gastrocnemius were 225 ± 43%, 240 ± 85%, and 278 ± 70%, respectively ($n = 4$), suggesting that the TC has a relatively short PEVK segment.

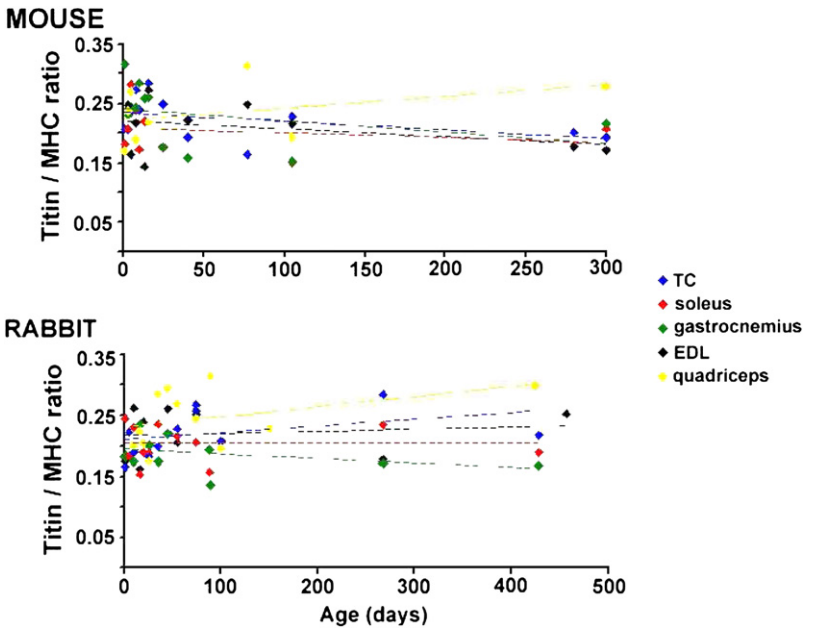

FIGURE 3 Titin expression, relative to MHC, as a function of age in murine and rabbit muscle. Data of each muscle was fitted with linear line. The obtained slopes were not significantly different from zero.

Passive stiffness increases during skeletal muscle development

The presence of additional PEVK sequences in neonatal skeletal muscle is predicted to result in lower titin-based stiffness, because of a reduced fractional extension of titin's extensible region for a given increase in sarcomere length. To examine the effect of upregulated PEVK exons on titin stiffness, we measured passive tension of skinned soleus and TC muscle dissected from neonatal (d5) and adult mice. Total passive tension was significantly lower in neonatal compared to adult muscle, in both soleus and TC (Fig. 6 *A*). Determining the collagen-based and the titin-based passive tension (see Methods) showed that the lower passive tension in neonatal skeletal muscle can be attributed to mainly lower titin-based passive tension (>50% reduced; this number was derived from the ratio of titin-based passive stiffness in neonatal muscle over titin-based stiffness in adult muscle) at all sarcomere lengths, with only a minor contribution from collagen that was only significant at the longer sarcomere lengths in soleus muscle (Fig. 6, *B* and *C*). Moreover, we also determined the stress-relaxation for 30 s while muscle length was held constant at the stretched length. The titin-based stress-relaxation phase was fit with a double-exponential decay function, and we found that the obtained time constants were not different between neonatal and adult skeletal muscle (soleus τ_1: 0.85 ± 0.06 vs. 0.75 ± 0.07 s^{-1}; τ_2: 10.5 ± 0.8 vs. 10.0 ± 0.7 s^{-1}, and TC τ_1: 0.77 ± 0.05 vs. 0.91 ± 0.05 s^{-1}; τ_2: 10.7 ± 0.2 vs. 10.7 ± 0.5 s^{-1}, d5 versus adult, respectively). The passive tension at the end of the 30-s hold was significantly lower in neonatal compared to adult skeletal muscle, in both soleus and TC, with the difference due to reduced titin-based passive tension (soleus: 20 ± 5 vs. 35 ± 4 mN/mm^2, and TC: 19 ± 7 vs. 61 ± 11 mN/mm^2, d5 versus adult, respectively). Thus, the mechanical studies revealed that during development, passive skeletal muscle becomes stiffer, due mainly to increased titin-based stiffness.

MARP expression changes during skeletal muscle development

MARPs are a family of muscle ankyrin repeat proteins that consists of CARP, Ankrd2, and DARP, all of which bind titin's N2A domain (27), located in the extensible region of titin directly proximal to the PEVK region. Recent work on MARP KO mice indicated that MARP expression might regulate titin isoform expression and passive properties of skeletal muscle (18). These findings prompted us to study MARP expression levels in neonatal and adult skeletal muscle. Western blotting showed in neonatal muscle increased expression (compared to adult mice) of Ankrd2 in gastrocnemius, but lower expression in soleus, with no change in TC. DARP expression was elevated in neonatal mice in both gastrocnemius and soleus muscle when compared to adults, again with no change in TC (Fig. 7). CARP expression was not detectable in adult skeletal muscle, in line with previous reports (28), and was also not detectable in neonatal skeletal muscle.

Inhibition of thyroid hormone secretion during skeletal muscle development

Previous work from our lab has shown that hypothyroidism in adult rats induces a switch from small adult cardiac titin back to large fetal titin isoforms, suggesting a role for thyroid hormones in regulating titin isoform expression (19). Subsequent in vitro studies also showed that the developmental

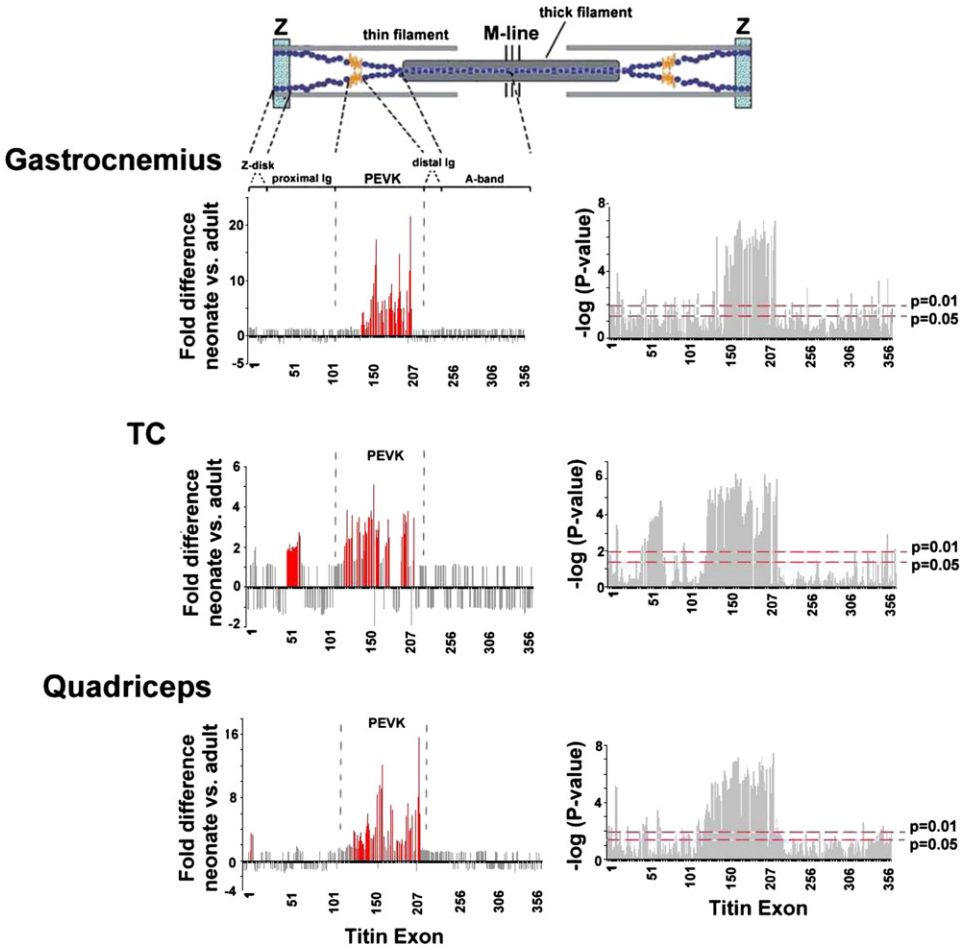

FIGURE 4 (*Left panels*) Titin exon composition of gastrocnemius, TC, and quadriceps muscle from neonatal (day 1) and adult mice. Exons >2-fold up- or downregulated are shown in red. Note the upregulation of PEVK exons in neonatal muscle. (*Right panels*) Bar graphs illustrating the statistical significance of the differences in exon composition between neonatal and adult skeletal muscle.

switch from large to smaller cardiac titin isoforms is regulated by thyroid hormones (17). These findings stimulated us to investigate the role of thyroid hormones in the titin isoform switch during in vivo skeletal muscle development. In line with previous work (29), serum concentrations of both T3 (active form) and T4 (prohormone, less active) were low at birth but increased rapidly with increasing age, peaking at ~16 days after birth. We achieved pharmacologically-induced congenital hypothyroidism by administrating MMI to the drinking water of pregnant mice starting at day 10 of gestation (24). (Note that MMI passes the placental barrier (29), unlike PTU that is used commonly in adult animals to cause hypothyroidism.) Neonatal mice stayed on MMI until 16 days after birth, at which time T3 levels were significantly decreased to ~50% of the concentration measured in non-treated mice (Fig. 8 *A*, *left panel*), and T4 levels were undetectable (<0.7 ng/dL; Fig. 8 *A*, *right panel*). This inhibition of thyroid hormone levels induced reexpression of neonatal MHC isoforms in skeletal muscle as well as beta myosin heavy chain isoforms in cardiac tissue (data not shown), which is in line with previous reports (19). Although 16-day control mice had rapidly changing skeletal muscle titin isoform expression (Fig. 2) and retarding the isoform switch should be most pronounced at this time, hypothyroidism did not significantly affect titin isoform expression in neither of the muscle types studied (Fig. 8 *B*). Thus, these findings do not support a major role for thyroid hormones in titin isoform switching during neonatal skeletal muscle development.

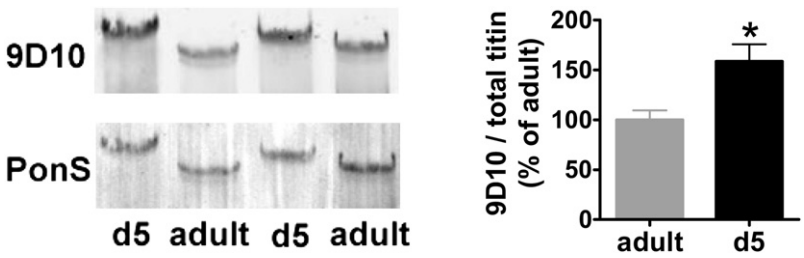

FIGURE 5 Western blotting studies on murine gastrocnemius with the PEVK-specific anti-titin antibody 9D10. (*Left panel*) Typical Western blot result with 9D10 labeling and PonceauS (PonS) staining of total titin. Note the stronger 9D10 labeling in neonatal (d5) versus adult gastrocnemius. (*Right panel*) Quantitative analysis of 9D10 labeling (normalized to protein levels obtained from the PonceauS membrane) in neonates as a percentage of labeling in adults. *Significantly different from adult, $p < 0.05$.

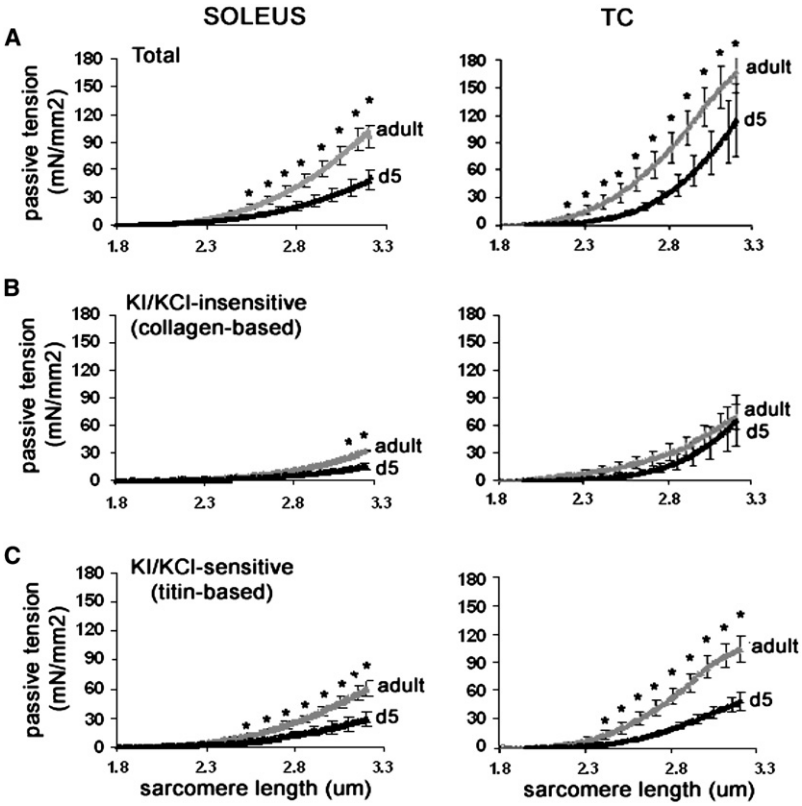

FIGURE 6 Passive mechanics of neonatal (d5) and adult murine skinned soleus and TC muscle. (*A*) Total passive tension as a function of sarcomere length. (*B*) Passive tension after extraction of thick and thin filaments with KCL/KI treatment (see Methods), defined as collagen-based passive tension. (*C*) Passive tension decrease after KI/KCl treatment, defined as titin-based passive tension. Note the significantly higher total passive tension and titin-based passive tension in adult muscle. *Significantly different from neonate, $p < 0.05$.

DISCUSSION

We used a multidisciplinary approach to address the role of titin in the change in skeletal muscle stiffness during postnatal development. Protein gels showed that skeletal muscles express large titin isoforms directly after birth, followed by a gradual switch toward progressively smaller isoforms. Titin exon microarray studies showed that reduced expression of exons coding for the extensible I-band region of titin, in particular PEVK exons, is an important contributor to this isoform switch. In line with these findings, muscle mechanics revealed that the increase of skeletal muscle stiffness during postnatal development is largely titin-based. Below we discuss these findings in detail.

Expression of a wide range of titin isoform sizes during neonatal skeletal muscle development

SDS-agarose studies showed that in various skeletal muscles from both mice and rabbits, titin isoform size decreases from large isoforms at birth to smaller isoforms in adults. We expected to see during development coexpression of large and small isoforms that remain of the same size but whose expression ratio shifts toward that of the adult, as observed in developing cardiac muscle (14–17). Instead, we observed on protein gels that neonatal skeletal muscle expresses a single titin band that gradually increases its mobility (mouse TC and quadriceps are the exception). This finding implies that during skeletal muscle development, many titin isoforms

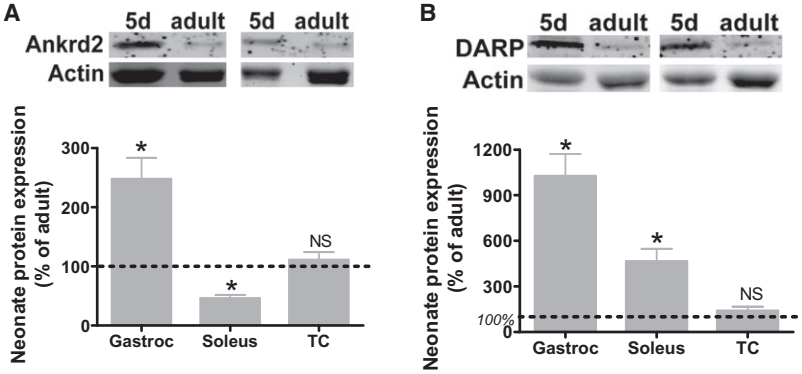

FIGURE 7 Expression of the MARP proteins (*A*) Ankrd2 and (*B*) DARP in neonatal and adult skeletal muscle from mouse. (*Top panels*) Typical Western blot results for Ankrd2 and DARP expression in m. gastrocnemius. Actin labeling shows protein loading. (*Bottom panels*) Both Ankrd2 (*A*) and DARP (*B*), normalized to actin, are upregulated in neonatal gastrocnemius and soleus muscle (except for Ankrd2 in soleus). Expression in TC was comparable between neonatal and adult muscle. *Significantly different from adult, $p < 0.05$.

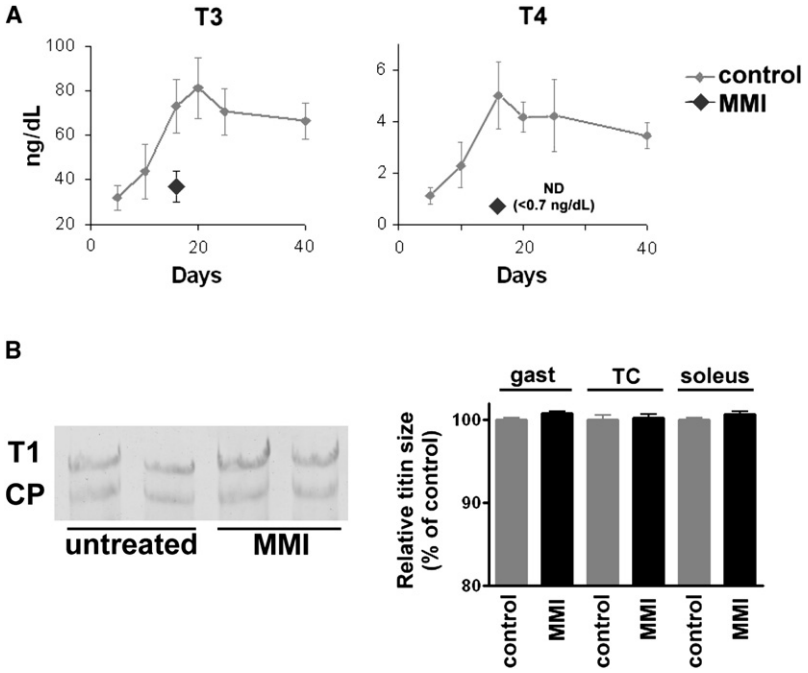

FIGURE 8 (*A*) Expression of thyroid hormones T3 and T4 as a function of age (*gray*). Note the reduction of T3 and T4 levels at day 16 (*black*) due to pharmacologically-induced congenital hypothyroidism through inhibition of thyroid hormone expression with MMI (added to the drinking water). ND, not detectable. (*B*) Hypothyroidism did not affect titin isoform switching in gastrocnemius, TC, and soleus of 16-day-old mice. (*Left*) Typical gel result of gastrocnemius. CP, chicken pectoralis titin (as mobility standard). (*Right*) Quantification of relative titin size in gastrocnemius (gast), TC, and soleus.

can be expressed that are close in mobility and that gradually shift from large to small. Titin exon microarray studies on neonatal and adult mouse muscles revealed that the decrease in titin isoform size during development is at least in part caused by restructuring of titin's extensible I-band region, in particular the PEVK segment (Fig. 3). Apparently, the number of splice pathways is not restricted to a few, but a large number of pathways exist in the PEVK region of the titin gene, thereby rendering titin isoforms that can differ several hundred kDa in size (Fig. 1 *D*). Thus, a remarkable restructuring of titin's spring region takes place during the first weeks after birth, replacing compliant neonatal titin isoforms with stiffer adult isoforms.

It should be noted that the reduction in titin molecular mass during development is ~200 kDa (Fig. 1 *B*), which exceeds the molecular mass of the differentially spliced exons (~150 kDa). An explanation for this discrepancy is that the gel-based decrease of titin molecular mass during development slightly overestimates the actual decrease, or likewise the microarray data might underestimate the actual decrease of molecular mass.

To analyze whether a pattern exists in the differential splicing of PEVK exons during development, we compared exon expression between different muscle types. Quadriceps, gastrocnemius, and TC show >2-fold upregulation of 61, 49, and 50 PEVK exons, respectively. Of the upregulated exons, two are specific to soleus, one is specific to gastrocnemius, and 14 exons are specific to TC. Thirty exons were upregulated across the three muscles types, all 30 (except one, exon 156) coding for the so-called PPAK repeats (12,30). Thus, during skeletal muscle development PPAK repeats appear to be spliced out of the titin molecule thereby increasing the proportion of E-rich motifs in the PEVK segment. The functional significance of this remains to be established, but considering that Ca^{2+} binding to E-rich motifs in the PEVK segment increases its bending rigidity (31) it could be speculated that a higher proportion of E-rich motifs in the PEVK segment elevates the Ca^{2+}-responsiveness of titin-based passive stiffness in adult muscle fibers. Furthermore, titin's PEVK domain has been shown to extend hierarchical on sarcomere stretch (32). This led Nagy et al. (32) to propose that PEVK-bound Ca^{2+} might dissociate gradually from titin's PEVK region driven by its magnitude of extension, thereby providing a means to monitor sarcomere length. Thus, increasing the proportion of Ca^{2+} binding E-rich motifs might sensitize this PEVK-based sensing of sarcomere stretch during skeletal muscle development. We propose that alternative splicing of titin during development renders stiffer titin isoforms with elevated Ca^{2+} responsiveness and that this improves fine motor control during muscle during development.

The fewer PEVK exons of adult titin will result in a shorter contour length of the extensible region, relative to that of neonatal titin, and as a result the fractional extension at a given sarcomere length will be higher. Because fractional extension is a main determinant of titin-based passive tension (33) adult titin is expected to be stiffer than neonatal titin. We tested this in both murine slow-twitch soleus and fast-twitch TC muscle. Across the sarcomere length range studied (~1.9–3.2 μm) titin was the major contributor to passive tension (soleus: 67% vs. 33% due to collagen; TC: 60% vs. 40% due to collagen), and this did not differ between adult and neonatal skeletal muscles. As predicted from the microarray studies, passive stiffness was

significantly larger at a wide range of sarcomere lengths in adult muscle, with most of the difference due to titin and only a minor role for collagen (Fig. 6). Overall, the increased titin-based passive tension during skeletal muscle development is consistent with the increase in stiffness during postnatal development that has been reported previously in cardiac muscle (14,16,34). Our work shows that the replacement of compliant titin with stiffer titin is a major factor that underlies the increase in titin-based stiffness during striated muscle development.

Mechanisms underlying the titin isoform switch during postnatal skeletal muscle development

Little is known regarding the molecular mechanisms driving titin isoform switching in striated muscle. Previous work in rat myocardium showed that hypothyroidism triggers a switch from small adult titin isoforms to large fetal isoforms (19). Moreover, Kruger et al. (17) showed that cultured cardiomyocytes respond to increased levels of thyroid hormones in the culture medium by switching from small cardiac titin isoforms to larger isoforms. Thus, we tested whether thyroid hormones are involved in the developmental titin isoform switch in skeletal muscle as well. We suppressed thyroid hormone production by >50% for T3 and >90% for T4 (further reduction in hormone levels resulted in a high death rate), which is considered severe hypothyroidism (35). Severe hypothyroidism is also suggested by our finding that MHC isoforms were switched toward fetal isoforms in skeletal muscle and β-MHC in murine LV muscle, a switch that is well established to occur in response to hypothyroidism (19,36). Despite the hypothyroidism we did not observe titin isoform switching in skeletal muscle. Thus, our results do not support a major role for thyroid hormones in titin isoform switching in skeletal muscle. As an alterative mechanism we studied the possible involvement of some of the structural and signaling proteins that are known to bind to titin. We focused on the proteins that bind to titin's extensible region and in particular the MARPs. Recent work suggested that MARPs (CARP, DARP, and Ankrd2), which bind to titin's N2A domain just proximal of the PEVK domain, are regulated by stretch and that this links titin-based myofibrillar stress/strain signals to a MARP-based regulation of muscle gene expression (27). Furthermore, a recent study by Barash et al. (18) showed that MARP-deficient skeletal muscle is less stiff and expresses large titin isoforms, and the authors suggested that MARPs might be involved in regulating titin isoform expression. These findings stimulated us to investigate MARP expression as a regulator of titin isoform switching during skeletal muscle development, and we hypothesized MARP expression to be upregulated during development. However, instead of upregulation during development we found general downregulation of both Ankrd2 and DARP (murine soleus and gastrocnemius muscle) or no change (TC). We confirmed previous reports that CARP expression was not detectable in adult or neonatal skeletal muscle (28). Thus, MARPs are unlikely to play a direct role in titin isoform switching and increased stiffness during muscle development. That titin isoform size in embryonic tissue was comparable to early neonatal tissue (see Fig. 2 *A*, murine quadriceps) suggests that titin isoform switching might be triggered by the increased muscle loading after birth. Clearly, unraveling the mechanisms driving alternative splicing of the titin gene needs further studies. Our finding of a gradual shift in titin isoform expression during development suggest that many splice pathways are possible, and that yet to be identified splice factors precisely fine-tune titin isoform characteristics to meet changes in mechanical load placed on skeletal muscle, such as occur during development.

CONCLUSION

Our work showed that during neonatal skeletal muscle development titin isoform size decreases, due mainly to restructuring of titin's I-band region, and in particular the PEVK region. Mechanical studies showed that titin isoform size reduction is a main contributor to the increase of muscle stiffness during skeletal muscle development. The underlying mechanisms are unlikely to involve thyroid hormone levels or changes in MARP expression. Titin stiffening, both in flexor and extensor muscles during neonatal development, likely contributes to stiffening of the musculo-tendon complex associated with postnatal development, and this is likely to be a significant factor in improving joint stability and motor control.

SUPPORTING MATERIAL

Methods, a figure, and references are available at http://www.biophysj.org/biophysj/supplemental/S0006-3495(09)01304-6.

We thank Ms. Diana Acuna, Ms. Luann Wyly, Mr. Eric Rogers, and Ms. Gem Stark, for expert technical assistance. We are especially grateful to Ms. Tiffany Pecor for her expert technical assistance with the microarray work.

This work was supported by a Rubicon postdoctoral grant from the Dutch Organization for Scientific Research (C.O.), and by the National Institutes of Health (HL062881 and HL084579 to H.G.).

REFERENCES

1. Schiaffino, S., and C. Reggiani. 1996. Molecular diversity of myofibrillar proteins: gene regulation and functional significance. *Physiol. Rev.* 76:371–423.
2. Lin, J. P., J. K. Brown, and E. G. Walsh. 1997. Soleus muscle length, stretch reflex excitability, and the contractile properties of muscle in children and adults: a study of the functional joint angle. *Dev. Med. Child Neurol.* 39:469–480.
3. Lebiedowska, M. K., and J. R. Fisk. 1999. Passive dynamics of the knee joint in healthy children and children affected by spastic paresis. *Clin. Biomech. (Bristol, Avon).* 14:653–660.

4. Nakagawa, Y., K. Hayashi, N. Yamamoto, and K. Nagashima. 1996. Age-related changes in biomechanical properties of the Achilles tendon in rabbits. *Eur. J. Appl. Physiol. Occup. Physiol.* 73:7–10.

5. Nakagawa, Y., T. Majima, and K. Nagashima. 1994. Effect of ageing on ultrastructure of slow and fast skeletal muscle tendon in rabbit Achilles tendons. *Acta Physiol. Scand.* 152:307–313.

6. Shadwick, R. E. 1990. Elastic energy storage in tendons: mechanical differences related to function and age. *J. Appl. Physiol.* 68:1033–1040.

7. Granzier, H. L., and T. C. Irving. 1995. Passive tension in cardiac muscle: contribution of collagen, titin, microtubules, and intermediate filaments. *Biophys. J.* 68:1027–1044.

8. Mutungi, G., J. Trinick, and K. W. Ranatunga. 2003. Resting tension characteristics in differentiating intact rat fast- and slow-twitch muscle fibers. *J. Appl. Physiol.* 95:2241–2247.

9. Granzier, H. L., and S. Labeit. 2004. The giant protein titin: a major player in myocardial mechanics, signaling, and disease. *Circ. Res.* 94:284–295.

10. Horowits, R., and R. J. Podolsky. 1987. The positional stability of thick filaments in activated skeletal muscle depends on sarcomere length: evidence for the role of titin filaments. *J. Cell Biol.* 105:2217–2223.

11. Trombitas, K., M. Greaser, S. Labeit, J. P. Jin, M. Kellermayer, et al. 1998. Titin extensibility in situ: entropic elasticity of permanently folded and permanently unfolded molecular segments. *J. Cell Biol.* 140:853–859.

12. Bang, M. L., T. Centner, F. Fornoff, A. J. Geach, M. Gotthardt, et al. 2001. The complete gene sequence of titin, expression of an unusual approximately 700-kDa titin isoform, and its interaction with obscurin identify a novel Z-line to I-band linking system. *Circ. Res.* 89:1065–1072.

13. Granzier, H., M. Radke, J. Royal, Y. Wu, T. C. Irving, et al. 2007. Functional genomics of chicken, mouse, and human titin supports splice diversity as an important mechanism for regulating biomechanics of striated muscle. *Am. J. Physiol. Regul. Integr. Comp. Physiol.* 293:R557–R567.

14. Lahmers, S., Y. Wu, D. R. Call, S. Labeit, and H. Granzier. 2004. Developmental control of titin isoform expression and passive stiffness in fetal and neonatal myocardium. *Circ. Res.* 94:505–513.

15. Kruger, M., T. Kohl, and W. A. Linke. 2006. Developmental changes in passive stiffness and myofilament Ca^{2+} sensitivity due to titin and troponin-I isoform switching are not critically triggered by birth. *Am. J. Physiol. Heart Circ. Physiol.* 291:H496–H506.

16. Warren, C. M., P. R. Krzesinski, K. S. Campbell, R. L. Moss, and M. L. Greaser. 2004. Titin isoform changes in rat myocardium during development. *Mech. Dev.* 121:1301–1312.

17. Kruger, M., C. Sachse, W. H. Zimmermann, T. Eschenhagen, S. Klede, et al. 2008. Thyroid hormone regulates developmental titin isoform transitions via the phosphatidylinositol-3-kinase/ AKT pathway. *Circ. Res.* 102:439–447.

18. Barash, I. A., M. L. Bang, L. Mathew, M. L. Greaser, J. Chen, et al. 2007. Structural and regulatory roles of muscle ankyrin repeat protein family in skeletal muscle. *Am. J. Physiol. Cell Physiol.* 293:C218–C227.

19. Wu, Y., J. Peng, K. B. Campbell, S. Labeit, and H. Granzier. 2007. Hypothyroidism leads to increased collagen-based stiffness and re-expression of large cardiac titin isoforms with high compliance. *J. Mol. Cell. Cardiol.* 42:186–195.

20. Warren, C. M., P. R. Krzesinski, and M. L. Greaser. 2003. Vertical agarose gel electrophoresis and electroblotting of high-molecular-weight proteins. *Electrophoresis.* 24:1695–1702.

21. Labeit, S., and B. Kolmerer. 1995. The complete primary structure of human nebulin and its correlation to muscle structure. *J. Mol. Biol.* 248:308–315.

22. Labeit, S., and B. Kolmerer. 1995. Titins: giant proteins in charge of muscle ultrastructure and elasticity. *Science.* 270:293–296.

23. Fukuda, N., Y. Wu, P. Nair, and H. L. Granzier. 2005. Phosphorylation of titin modulates passive stiffness of cardiac muscle in a titin isoform-dependent manner. *J. Gen. Physiol.* 125:257–271.

24. Sole, E., R. Calvo, M. J. Obregon, and A. Meseguer. 1996. Effects of thyroid hormone on the androgenic expression of KAP gene in mouse kidney. *Mol. Cell. Endocrinol.* 119:147–159.

25. Trombitas, K., M. Greaser, G. French, and H. Granzier. 1998. PEVK extension of human soleus muscle titin revealed by immunolabeling with the anti-titin antibody 9D10. *J. Struct. Biol.* 122:188–196.

26. Wang, S. M., and M. L. Greaser. 1985. Immunocytochemical studies using a monoclonal antibody to bovine cardiac titin on intact and extracted myofibrils. *J. Muscle Res. Cell Motil.* 6:293–312.

27. Miller, M. K., M. L. Bang, C. C. Witt, D. Labeit, C. Trombitas, et al. 2003. The muscle ankyrin repeat proteins: CARP, ankrd2/Arpp and DARP as a family of titin filament-based stress response molecules. *J. Mol. Biol.* 333:951–964.

28. Ishiguro, N., T. Baba, T. Ishida, K. Takeuchi, M. Osaki, et al. 2002. Carp, a cardiac ankyrin-repeated protein, and its new homologue, Arpp, are differentially expressed in heart, skeletal muscle, and rhabdomyosarcomas. *Am. J. Pathol.* 160:1767–1778.

29. McArdle, A., T. R. Helliwell, G. J. Beckett, M. Catapano, A. Davis, et al. 1998. Effect of propylthiouracil-induced hypothyroidism on the onset of skeletal muscle necrosis in dystrophin-deficient mdx mice. *Clin. Sci. (Lond.).* 95:83–89.

30. Greaser, M. 2001. Identification of new repeating motifs in titin. *Proteins.* 43:145–149.

31. Labeit, D., K. Watanabe, C. Witt, H. Fujita, Y. Wu, et al. 2003. Calcium-dependent molecular spring elements in the giant protein titin. *Proc. Natl. Acad. Sci. USA.* 100:13716–13721.

32. Nagy, A., L. Grama, T. Huber, P. Bianco, K. Trombitas, et al. 2005. Hierarchical extensibility in the PEVK domain of skeletal-muscle titin. *Biophys. J.* 89:329–336.

33. Watanabe, K., P. Nair, D. Labeit, M. S. Kellermayer, M. Greaser, et al. 2002. Molecular mechanics of cardiac titin's PEVK and N2B spring elements. *J. Biol. Chem.* 277:11549–11558.

34. Opitz, C. A., M. C. Leake, I. Makarenko, V. Benes, and W. A. Linke. 2004. Developmentally regulated switching of titin size alters myofibrillar stiffness in the perinatal heart. *Circ. Res.* 94:967–975.

35. Mortoglou, A., and H. Candiloros. 2004. The serum triiodothyronine to thyroxine (T3/T4) ratio in various thyroid disorders and after Levothyroxine replacement therapy. *Hormones (Athens).* 3:120–126.

36. Tang, Y. D., J. A. Kuzman, S. Said, B. E. Anderson, X. Wang, et al. 2005. Low thyroid function leads to cardiac atrophy with chamber dilatation, impaired myocardial blood flow, loss of arterioles, and severe systolic dysfunction. *Circulation.* 112:3122–3130.